Nat Hazards (2012) 64:707–728
DOI 10.1007/s11069-012-0265-7

ORIGINAL PAPER

Probabilistic assessment of wildfire hazard and municipal watershed exposure

Joe Scott · Don Helmbrecht · Matthew P. Thompson · David E. Calkin · Kate Marcille

Received: 5 April 2012 / Accepted: 20 June 2012 / Published online: 12 July 2012

Abstract The occurrence of wildfires within municipal watersheds can result in significant impacts to water quality and ultimately human health and safety. In this paper, we illustrate the application of geospatial analysis and burn probability modeling to assess the exposure of municipal watersheds to wildfire. Our assessment of wildfire exposure consists of two primary components: (1) wildfire hazard, which we characterize with burn probability, fireline intensity, and a composite index, and (2) geospatial intersection of watershed polygons with spatially resolved wildfire hazard metrics. This effort enhances investigation into spatial patterns of fire occurrence and behavior and enables quantitative comparisons of exposure across watersheds on the basis of a novel, integrated measure of wildfire hazard. As a case study, we consider the municipal watersheds located on the Beaverhead-Deerlodge National Forest (BDNF) in Montana, United States. We present simulation results to highlight exposure across watersheds and generally demonstrate vast differences in fire likelihood, fire behavior, and expected area burned among the analyzed municipal watersheds. We describe how this information can be incorporated into risk-based strategic fuels management planning and across the broader wildfire management spectrum. To conclude, we discuss strengths and limitations of our approach and offer potential future expansions.

Keywords Wildfire · Hazard analysis · Exposure analysis · Fire modeling · Municipal watersheds

J. Scott
Pyrologix LLC, Missoula, MT 59801, USA

D. Helmbrecht
TEAMS Enterprise Unit, US Forest Service, Missoula, MT 59807, USA

M. P. Thompson (✉) · D. E. Calkin
Rocky Mountain Research Station, US Forest Service, Missoula, MT 59807, USA
e-mail: mpthompson02@fs.fed.us

K. Marcille
Oregon State University, Corvallis, OR 97331, USA

1 Introduction

In this paper, we illustrate the application of geospatial analysis and burn probability modeling to assess wildfire hazard and exposure of municipal watersheds (i.e., drinking water supplies) to wildfire. Wildfires can have profound effects on watersheds (Parise and Cannon 2012), and sediment loads from burned watersheds have resulted in shutdowns of municipal water supply facilities due to water quality (Ryan and Samuels 2010). Thus, there are pressing human health and safety reasons for identifying at-risk watersheds. As a case study, we consider the municipal watersheds located on the Beaverhead-Deerlodge National Forest (BDNF) in Montana, United States. Our assessment of wildfire exposure consists of two primary components: (1) wildfire hazard, which we characterize with burn probability, fireline intensity, and a composite index, and (2) geospatial intersection of watershed polygons with spatially resolved wildfire hazard metrics.

1.1 Background: wildfire hazard and risk analysis

Federal wildfire management within the United States is increasingly adopting risk-based paradigms to inform policy and management (Calkin et al. 2011a; Fire Executive Council 2009). Recently published examples include strategic national-scale assessments (Thompson et al. 2011a), fuel treatment evaluation (Ager et al. 2010), incident-level decision support (Calkin et al. 2011b; Noonan-Wright et al. 2011), and localized assessment of risk to structures in the wildland–urban interface (Bar Massada et al. 2009). Advancements in computing power, fire behavior modeling, and geospatial data acquisition and management enable spatially explicit simulation of where fire is likely to ignite, spread, and interact with highly valued resources and assets (Finney et al. 2011; Finney 2002). Applications of burn probability modeling techniques are still emerging, with enormous potential for risk-based, strategic fire and fuels management (Miller et al. 2008).

Wildfire hazard is defined here as a physical situation with the potential for wildfire to cause damage. Qualitatively, hazard can be described by the fire environment surrounding the resource, for instance the fuel, weather, topography, and ignition characteristics. Quantitatively, hazard can be described as the probability distribution of a fire characteristic, usually wildfire intensity. A location likely to burn with high intensity, in this modeling approach, has high hazard. Hazard, however, is but one component of wildfire risk. Finney (2005) provides a quantitative definition of wildfire risk that integrates information on burn likelihood, fire intensity, and magnitude of resource response to fire. This approach aligns with ecological risk assessment paradigms premised on the analysis of exposure and effects (Fairbrother and Turnley 2005). Wildfire exposure analysis typically explores the possible spatial interactions of fire-susceptible resources with fire occurrence and behavior metrics, and fire effects analysis explores the potential magnitude of wildfire-caused damages (Thompson and Calkin 2011). Conversely, for fire-adapted ecosystems, exposure and effects analysis could highlight where fire may play an ecologically beneficial role and be promoted. Assessing risk informs decision making by integrating and synthesizing information regarding the likelihood and magnitude of impacts to resources (Sikder et al. 2006). This information can be used to help plan risk mitigation activities across the wildfire management spectrum, including ignition prevention efforts, proactive hazardous fuels reduction, suppression response planning, and evacuation planning (Dennison et al. 2007).

1.2 Wildfire impacts to watershed health and integrity

Watersheds play important ecological, social, and economic roles and can potentially be affected by a multitude of human and natural disturbances (Brauman et al. 2007; Brown 2000; Neary et al. 2005). Consideration of watershed health and integrity across the forest is important for numerous reasons. Forests and federal lands, particularly in the Western United States, are important providers of the water supply (Brown et al. 2008; Ryan and Samuels 2010). Ecologically, watersheds have the potential to be greatly impacted by wildland fire, and the results are often far-reaching. The natural occurrence of fire on the landscape is an important component of watershed health and may have beneficial effects in the long run (e.g., increased biodiversity) and functions as an agent of recovery (Benda et al. 2003). However, fire can also induce dramatic and negative changes to watershed integrity through flooding, debris flow, and subsequent impacts on human lives and species' habitat suitability. Post-fire effects can range in magnitude and impact, across time and space, from rejuvenation of alluvial fans to burial of existing habitat (Benda et al. 2003). Post-fire floods and high sediment flow are of high concern (Neary et al. 2005). Areas that have been naturally disturbed (i.e., post-fire environment) become more susceptible to substantial human degradation (Brown and Binkley 1994).

Erosion and sediment redistribution are commonly referenced as prominent effects of fire on watersheds (Brown and Froemke 2010; Calkin et al. 2007; Shakesby and Doerr 2006; Brown 2000; Brown and Binkley 1994; Agee 1993). Stand-replacing fires (high severity) often result in intense erosion and large influxes of sediment (Benda et al. 2003) and woody debris in stream channels and confluences (Neary et al. 2005; Benda et al. 2003; Brown 2000) as well as shift overland flow rates and runoff behavior (Shakesby and Doerr 2006). Debris flows are a potential response of recently burned basins and are considered more severe than sediment-laden floods (Cannon et al. 2010). Fire severity is a major determinant of impacts to soil and water resources (Shakesby and Doerr 2006; Neary et al. 2005).

Our interest here is in wildfire impacts as they relate to municipal watersheds; readers wishing for a more thorough review of hydrologic, geomorphic, and aquatic habitat-related effects of wildfire are referred to Parise and Cannon (2012), Rieman et al. (2010), Moody and Martin (2009), Dunham et al. (2007), Shakesby and Doerr (2006), Neary et al. (2005), and Bisson et al. (2003). Municipal watersheds are critical infrastructure and disruption of their operation can have serious economic and public safety consequences (Ryan and Samuels 2010); hence, their explicit consideration within decision support systems supporting incident management (Calkin et al. 2011b) and within strategic risk assessments (Thompson et al. 2011a, b). Municipal water is affected by wildland fire occurrence and management practices associated with fire (Brown 2000). Threats to drinking water from wildfire are varied and can occur while a fire burns, from aerial application of fire retardant (Neary et al. 2005; Ryan and Samuels 2010), or in the months and years following a fire due to increased storm runoff (Shakesby and Doerr 2006), ash accumulation, and accelerated soil erosion and sedimentation (Emelko et al. 2011; Smith et al. 2010).

1.3 Case study description: BDNF wildfire hazard assessment

The study area for the assessment of watershed exposure included the approximately 3.2 million ha (8 million acres) in 12 BDNF planning units (called "landscapes" in the Forest plan; see Fig. 1). The study area is less fire-prone than many other landscapes in the western United States, but wildfire is nevertheless a concern. Our analysis sought to understand spatial patterns in hazard due to large fires. For this analysis, we defined a "large fire" as one greater than 121.41 ha (300 ac) in final fire size, consistent with USDA Forest Service accounting and reporting procedures. Across the years 1992–2009, large fires accounted for only 2.55 % of all fire occurrences, while accounting for 94.49 % of all area burned. This result is consistent in other areas of the western United States as well, where area burned is largely driven by large fire spread rather than localized ignitions. By incorporating information on total area burned relative to the area covered by burnable vegetation within the study area (exclusive of water, rock, urban areas, etc.) and dividing by the number of years analyzed, we derived a non-spatial average annual burn probability of 0.001196 across the study area.

With this study, we quantify wildfire exposure to the 10 municipal watersheds on the BDNF. Explicit identification of municipal watersheds is a sensitive, national security issue due to the potential serious consequences of disruption. Therefore, exact names and locations of municipal watersheds across the landscapes will not be provided. Instead, we refer to the municipal watersheds by code letter (A through J) and identify the landscape in which each watershed is located (Table 1).

The municipal watersheds vary in several important characteristics that may affect their wildfire exposure (Table 1). The upper reaches of many of the watersheds extend into bare ground at ridge tops. Watershed area covered by burnable vegetation (Table 1; column e) ranges from a low of 58.8 % (watershed C) to a high of 99.5 % (J). Spatial variability in ignition likelihood, fuel conditions, and terrain jointly influence spatial patterns of potential fire spread and municipal watershed exposure. The spatial patterns of ignitions in particular may be an important factor affecting burn probability (Bar Massada et al. 2011). The ignition density grids we used (see Sect. 2) quantify historical wildfire occurrence on a relative basis across grid cells of equal area. To quantify relative ignition likelihood across watersheds, we summed ignition density values from grid cells within each watershed. This derived metric, relative ignition density (Table 1; column f) provides a comparison of the likelihood that a wildfire will start within each watershed (per unit area), scaled to the watershed with the highest ignition density (Watershed G, in the Clark Fork-Flints landscape). Watersheds D and I, also in the Clark Fork-Flints landscape, have the second- and third-highest ignition density at 89.4 and 66.3 % of the maximum, respectively. By comparison, the relative ignition density of all remaining watersheds ranges from 49.5 to 65.8 %.

2 Methods

The primary model we used is the FSim large-fire simulator (Finney et al. 2011). FSim is a spatially explicit model that pairs existing fire growth models (Finney 1998, 2002) and a model of large-fire ignition probability with artificially generated weather streams in order to simulate fire ignition and growth for thousands of fire seasons. FSim does not modify landscape conditions through time to reflect disturbance or succession, and thus each simulation is a possible realization of a single fire season given current conditions. These simulations are used to estimate annual burn probability (BP), mean fireline intensity (MFI), and fire-size distributions. FSim annual burn probabilities are fundamentally different from other work presenting conditional burn probabilities (e.g., Ager et al. 2010); FSim explicitly models the likelihood of large-fire ignitions, which on some landscapes may be quite infrequent, whereas the latter approach models burn probabilities conditional on an ignition occurring. The simulated weather sequences combine time series analysis of

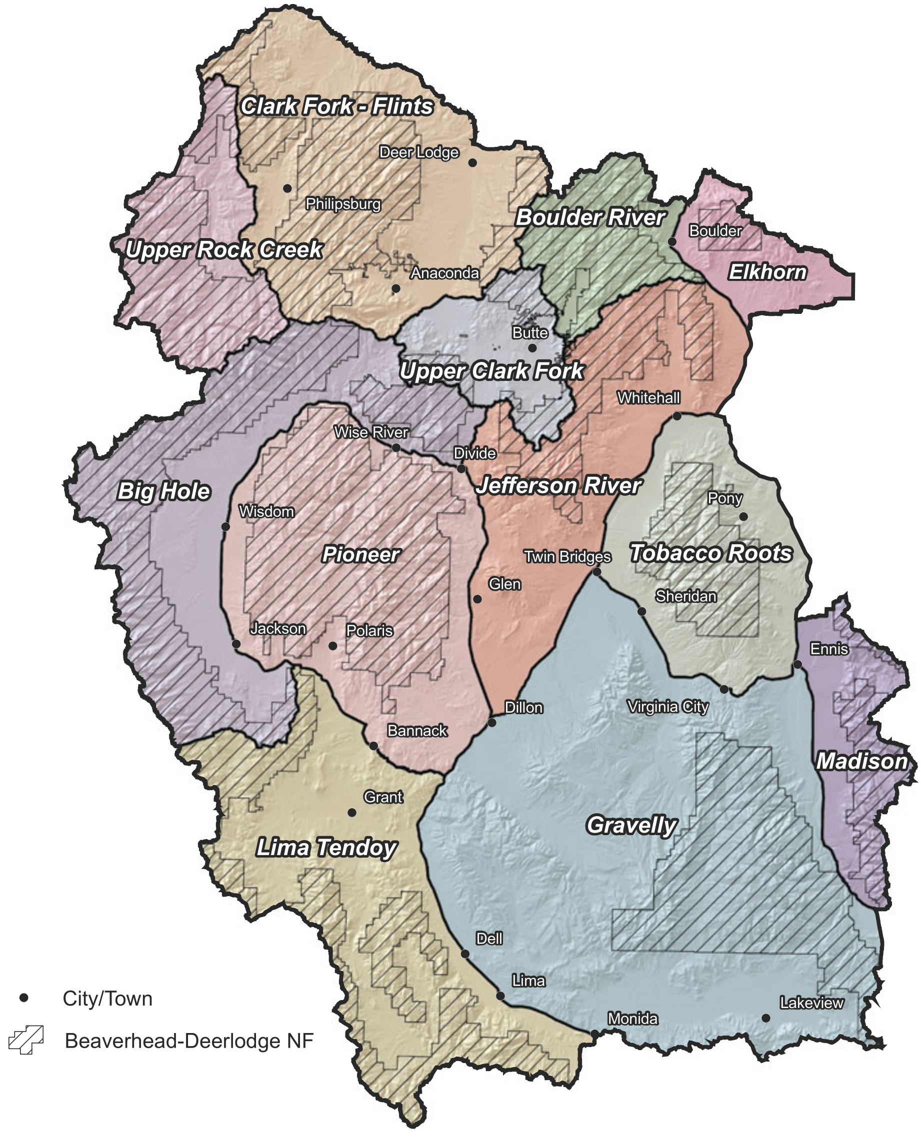

Fig. 1 Overview of the analysis area for the assessment of wildfire hazard and watershed exposure on the Beaverhead-Deerlodge National Forest, showing 12 planning units ("landscapes" as identified in the Forest plan), listed alphabetically: Big Hole, Boulder River, Clark Fork-Flints, Elkhorn, Gravelly, Jefferson River, Lima-Tendoy, Madison, Pioneer, Tobacco Roots, Upper Clark Fork, and Upper Rock Creek. The 10 municipal watersheds of interest are found across these 12 BDNF landscapes (Table 1). National Forest System lands are shown in cross-hatching

the fire danger rating index Energy Release Component (ERC) and corresponding fuel moisture scenario with historic joint distributions of wind speed and direction. For use in FSim, empirical distribution functions that relate daily ERC values to large-fire occurrence for the fire modeling area were developed in FireFamilyPlus (Rocky Mountain Research Station Fire Sciences Laboratory and Systems for Environmental Management 2002). Fire

Table 1 Characteristics of the ten municipal watersheds on the Beaverhead-Deerlodge National Forest

(a) Watershed	(b) BDNF landscape	(c) Total watershed area (ha)	(d) Burnable watershed area (ha)	(e) Burnable area (% of total watershed)	(f) Relative ignition density (%)
A	Boulder River	10,779	10,093	93.6	60.3
B	Upper Clark Fork	3,144	3,115	99.1	54.6
C	Jefferson River	885	521	58.8	52.5
D	Clark Fork-Flints	788	722	91.6	89.4
E	Tobacco Roots	3,021	2,494	82.5	65.8
F	Pioneer	6,425	5,930	92.3	58.3
G	Clark Fork-Flints	1,593	1,580	99.2	100.0
H	Big Hole	1,290	1,264	98.0	49.5
I	Clark Fork-Flints	1,812	1,303	71.9	66.3
J	Upper Clark Fork	1,337	1,330	99.5	57.5

Non-burnable watershed area consists of bare ground at the upper reaches of the watersheds. Relative ignition density (column f) is an indicator of the relative potential for fire starts within the watersheds. Because the ignition density grid used to produce these data is coarse (see Fig. 2), relative ignition density in the area surrounding the watersheds should be similar to the values reported here

duration is not fixed within FSim, but rather is determined by the artificially generated weather stream and an embedded suppression algorithm (Finney et al. 2009).To minimize edge effects, we allowed simulated fires to move into the analysis area from adjacent land by including a 8-km (5-mile) buffer from the edge of any landscape to the extent of our geospatial data. The total fire modeling area encompasses 6,103,188 ha (15,080,978 acres), and using a 90 m pixel resolution, this resulted in a modeling landscape of 2,415 $\times$ 3,120 pixels.

Figure 2 presents a simplified flowchart for our wildfire exposure analysis process, with the key analytical steps highlighted in gray. In the following subsections, we describe our methods for creating the necessary input files for FSim and for performing the wildfire exposure analysis with FSim. Specifically, this entailed generating information on landscape characteristics such as terrain and fuel conditions (§2.1), acquiring weather data for generating artificial fire seasons (§2.2), obtaining fire occurrence data and developing probabilistic large-fire occurrence relationships (§2.3), and running the model to characterize pixel-based wildfire hazard within municipal watersheds (§2.4).

2.1 Generation of landscape file for fire simulation model

In order to simulate fire growth and behavior, FSim requires a user-defined landscape file, which consists of geospatial data representing terrain, fuel, and vegetation characteristics. Terrain characteristics include slope steepness, aspect, and elevation. Fuel characteristics include surface fire behavior fuel model, forest canopy base height, and forest canopy bulk density. Vegetation characteristics include forest canopy cover and forest canopy height. LANDFIRE (www.landfire.gov) is a valuable source for such data; however, a few challenges existed when applying LANDFIRE's off-the-shelf landscape data for this mid-scale assessment. First, the fire modeling area includes portions of four LANDFIRE mapping zones, resulting in data discontinuities (seamlines) at mapping zone boundaries. This occurred if the LANDIFRE rules for assigning and mapping fuel characteristics (i.e.,

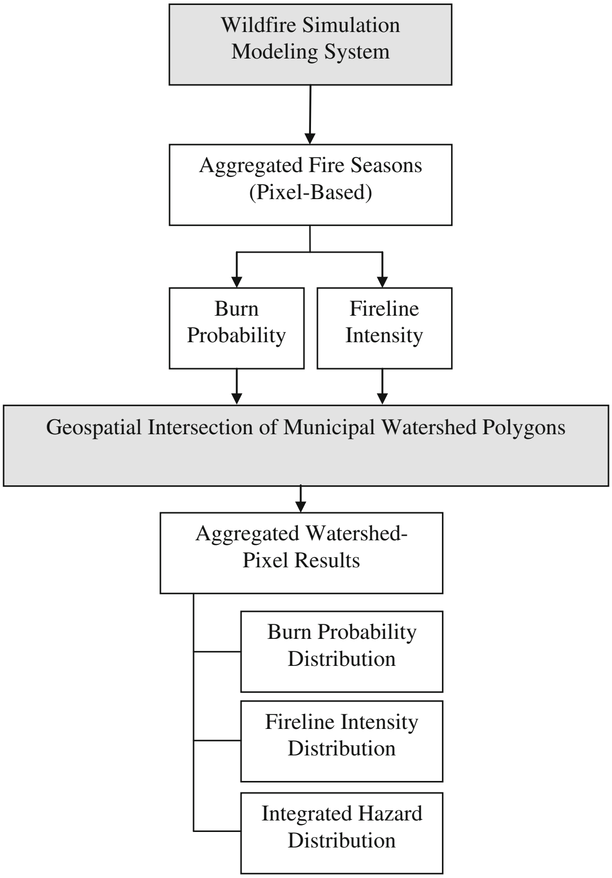

Fig. 2 Simplified flowchart for wildfire exposure analysis process. *Highlighted* in *gray* are the key analytical steps, with the most effort involved in wildfire simulation. Pixel-based wildfire hazard metrics are intersected with HVRA polygons to provide multiple characterizations of HVRA exposure to wildfire

surface fire behavior fuel model, canopy base height, and canopy bulk density) differed between zones. Rules for mapping fuel characteristics are based on the combinations of existing vegetation type (EVT), existing vegetation cover (EVC), existing vegetation height (EVH), and biophysical setting (BpS). Second, rules for mapping fuel characteristics are generalized to whole LANDFIRE mapping zones, which span millions of hectares each. Rules that account for variability across a whole mapping zone can result in imprecision when looking at just a small portion of the mapping zone. Third, LANDFIRE's published forest canopy cover data available at the time were known to overestimate this factor (this overestimate has since been corrected and is not present in recent versions of LANDFIRE data).

For these reasons, we held a local fuel calibration workshop with BDNF fire and fuel staff to produce seamless, locally calibrated surface and canopy fuel data based on LANDFIRE data version 1.0.0 of EVT, EVC, EVH, and BpS. A local calibration workshop provides the opportunity for fire and fuels staff to critique and "fine-tune" the LANDFIRE data for use at a more local scale based on their collective experience and knowledge of the area. The data sets can also be updated to reflect recent disturbances such as wildfire and insect outbreaks. We took slope, aspect, and elevation from LANDFIRE version 1.0.0 (LANDFIRE "National") without adjustment. We also used LANDFIRE version 1.0.0 data, without adjustment, for vegetation height and cover of shrub and grass lifeforms. We reduced vegetation cover of the tree lifeform (forest canopy cover) using the recommended procedure posted on the LANDFIRE Web site (LANDFIRE 2010).

At the local calibration workshop, we reviewed, and edited where necessary, the LANDFIRE fuel mapping rules to create a geospatial layer of surface fire behavior fuel models. We used the LANDFIRE National EVC layer for herbaceous and shrub lifeforms, but substituted our adjusted canopy cover values for the tree lifeform. This calibration process produced a fuel model layer valid as of ca. 2000, the year of the imagery used by LANDFIRE to produce the geospatial vegetation data.

To generate the canopy bulk density layer, we used a general linear model (GLM) produced by LANDFIRE (Reeves et al. 2009), which is now used in LANDFIRE versions 1.0.5 (Refresh 2001) and 1.1.0 (Refresh 2008). The GLM is essentially a nonlinear regression of canopy bulk density against forest canopy cover and height, based on data from the LANDFIRE Reference Database (LFRDB) (LANDFIRE 2010). To generate the canopy base height layer, we used a new mapping method produced by LANDFIRE. Like the GLM for canopy bulk density, this canopy base height mapping method is now used in LANDFIRE versions 1.0.5 and 1.1.0 data. It is also available in the newly released Total Fuel Change Tool developed by the LANDFIRE program (LANDFIRE 2010).

To update the landscape model to vegetation conditions in 2009, we needed to reflect fuel changes associated with wildfires that occurred between 2000 and 2009. Using fire severity data from the Monitoring Trends in Burn Severity (MTBS) program (MTBS 2010), we identified areas that experienced a wildfire during that time period. We worked with BDNF fire and fuel staff to create expert-opinion rules that identified a post-fire fuel model as a function of EVT, fire severity (three classes), and time since fire occurrence (1–5 years and 6–10 years). Forest canopy height was assumed to remain unchanged after low and moderate severity fire; canopy cover and canopy bulk density were reduced to a specified fraction of the pre-fire level. All canopy characteristics were set to zero in the case of high-severity fire, on the assumption that a high-severity fire would effectively remove the entire forest canopy.

It was further necessary to update the landscape model conditions to reflect changes due to the beetle infestation. A procedure similar to the wildfire update was used. In place of the MTBS fire severity data used for the wildfire update, we used geospatial data representing relative overstory canopy loss produced by the US Forest Service Region 1 Geospatial Services Group. Their data classified the relative amount of canopy cover reduction from 2000 to 2009 (Ahl et al. 2010). We created an expert-opinion lookup table based on the pre-infestation fuel model and relative canopy loss class to estimate the surface fuel model as of 2009. We left canopy height and canopy base height unchanged following the outbreak, assuming that the beetles would not affect the smaller trees that contribute most to canopy base height. We reduced canopy bulk density and canopy cover in direct proportion to the Region 1 canopy loss values.

The effects of insect infestations on fuel and fire behavior vary with time since disturbance (Simard et al. 2011; Page and Jenkins 2007a, b; Jenkins et al. 2008). Very early in the infestation, during the "red phase" of an infestation, the surface fuel model and most canopy characteristics remain unchanged, but the reduced moisture content of the dead and dying foliage may temporarily increase the potential for crown fire. We did not simulate this phase because it is of relatively short duration at any given place on the landscape, usually less than 3 years. The lag time between measurement of canopy loss and assessment of wildfire hazard means that red-phase stands will likely have moved into the longer-duration gray phase. Instead, we simulated the longer-duration standing-gray phase during which the foliage and fine branches of dead trees have fallen to the ground—so canopy bulk density is reduced and surface fuel load is slightly increased—but the dead trees remain standing with much of their branchwood still attached. Decades after the outbreak, these dead trees will be falling to the ground, exacerbating fuel consumption, smoke production, and resistance to control in the event of a wildfire. We did not simulate this later phase of the current outbreak.

2.2 Fire weather

We identified five representative weather stations from across the forest with consistent hourly wind and daily fire weather observations. Using FireFamilyPlus (Rocky Mountain Research Station Fire Sciences Laboratory and Systems for Environmental Management 2002), we calculated the seasonal trend in the daily mean and standard deviation of ERC throughout a calendar year. This information is used by FSim to produce artificial ERC traces for a season. Also using FireFamilyPlus, we generated monthly joint distributions of wind speed and direction. This information is used by FSim to randomly draw a wind speed and direction, independently for each day of a simulation.

2.3 Fire occurrence

FSim requires information regarding the historic occurrence of fire in the analysis area, specifically large fires—those that escape initial attack and require an extended attack suppression response. We gathered fire occurrence data for all jurisdictions in the analysis area. A total of 82 large fires occurred in the analysis area between 1990 and 2009; those fires started on 65 days (that is, some days had multiple fire starts). We used FireFamilyPlus to estimate the coefficients of a logistic regression model of the probability of a large-fire day within the 15 million acre fire modeling area. A large-fire day is a day on which one or more fires start (or is discovered) that eventually burns more than 300 acres. FSim uses these regression coefficients to simulate the ignition of large fires based on simulated weather.

We also determined the distribution of number of fires started on each of the 65 large-fire days. During the last 19 years on the fire modeling area, only one large fire started on 58 of the 65 large-fire days in the record (89 %), two fires started on 5 of the days, four on one day (July 23, 2000), and ten started on one day (July 31, 2000).Past fire start locations have not been uniform across the fire modeling area. To account for that non-uniformity, FSim uses a geospatial layer indicating relative ignition density across the landscape and randomly locates fires according to this density grid. The ignition locations of all 82 large fires in the analysis area are shown in Fig. 3. Because FSim is concerned only with large fires, which occur relatively infrequently on the landscape, we used a nationwide large-fire ignition density grid created at the Missoula Fire Sciences Laboratory based on a 75 km average density (and a cell size of 20 km). The highest density of large-fire starts is found in the NW corner of the analysis area (Fig. 3). The southeast corner has a moderate density of large-fire starts. The lowest density of large-fire starts occurs along a southwest to northeast line running though the

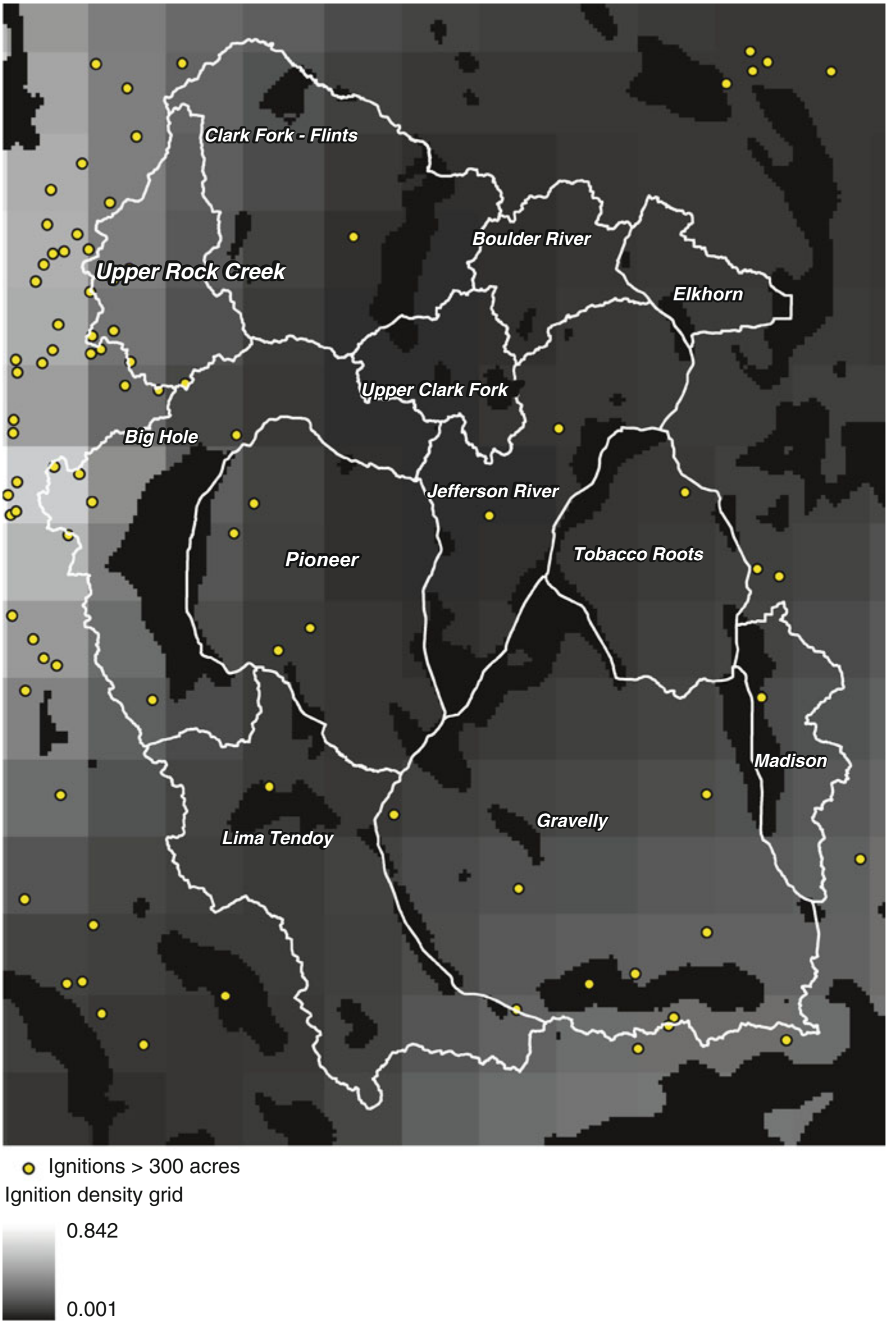

Fig. 3 Start locations of fires greater than 121.41 ha (300 acres) (*yellow dots*) that occurred 1990–2009, and the relative ignition density grid (unit-less) created from such locations at a nationwide scale. The ignition density grid is used in FSimto locate simulated fires across the landscape. This grid helps explain the variability of burn probability across the landscape. To prevent FSim from starting large fires in valley-bottom locations, we created a valley-bottom mask and artificially lowered the ignition density in those locations to an arbitrarily small nonzero value

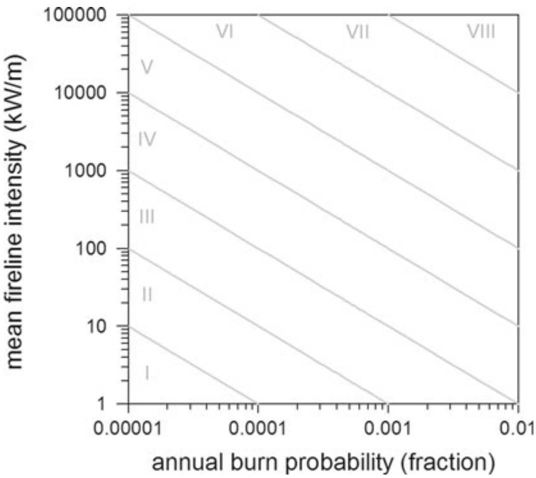

Fig. 4 A wildfire hazard characteristics chart illustrating integrated hazard through diagonal lines representing the product of BP and MFI. This hazard characterization sorts individual landscape pixels into integrated wildfire hazard classes, I–VIII. Pixels with high BP and high MFI have high wildfire hazard; pixels with low BP and low MFI have low wildfire hazard

center of the analysis area. On a highly variable landscape like the BDNF, which includes forested mountains and grassland valley bottoms, such a coarse-scale ignition density grid tends to wash out the fine-scale patterns that occur. In this case, the supplied ignition density grid indicates a higher propensity to start large fires in the valley-bottom grasslands than the historic locations would indicate appropriate. In lieu of developing a custom classification and regression tree model or logistic regression specifically for this analysis, we instead simply identified the valley-bottom grasslands within the fire modeling area and set the ignition probability to an arbitrarily low value (0.001).Fires ignited outside the valley bottoms could still burn into and across them if supported by fuel conditions.

2.4 Pixel-based wildfire hazard and exposure

Upon completion of preparatory work, we used FSim to simulate 40,000 fire seasons using a pixel resolution of 90 m. We quantified wildfire hazard across the BDNF with two primary, pixel-level FSim results: burn probability (BP) and mean fireline intensity (MFI). Burn probability is the annual probability that an individual landscape pixel will experience a wildfire, calculated as the number of times a pixel is burned during any of the iterations divided by 40,000 (the total number of iterations). Mean fireline intensity is the arithmetic mean fireline intensity (kW/m) of the simulation iterations that burned each pixel. These two factors taken together characterize wildfire hazard at a pixel. For a single measure of integrated wildfire hazard, we multiply these two results together and bin into eight mutually exclusive hazard classes. A wildfire hazard assessment chart (Fig. 4) illustrates this integrated hazard measure as diagonal lines (on a log–log scale) representing lines of equal integrated hazard. Pixels with high BP and high MFI fall in the highest integrated wildfire hazard class; pixels with low BP and low MFI fall in the lower classes. To characterize exposure, we summarized BP, MFI, and integrated hazard metrics across all landscape pixels within watershed polygon boundaries. Based on these pixel-level results, we calculated the expected annual watershed area burned by multiplying the watershed-mean BP (excluding non-burnable pixels) by the burnable area of the watershed.

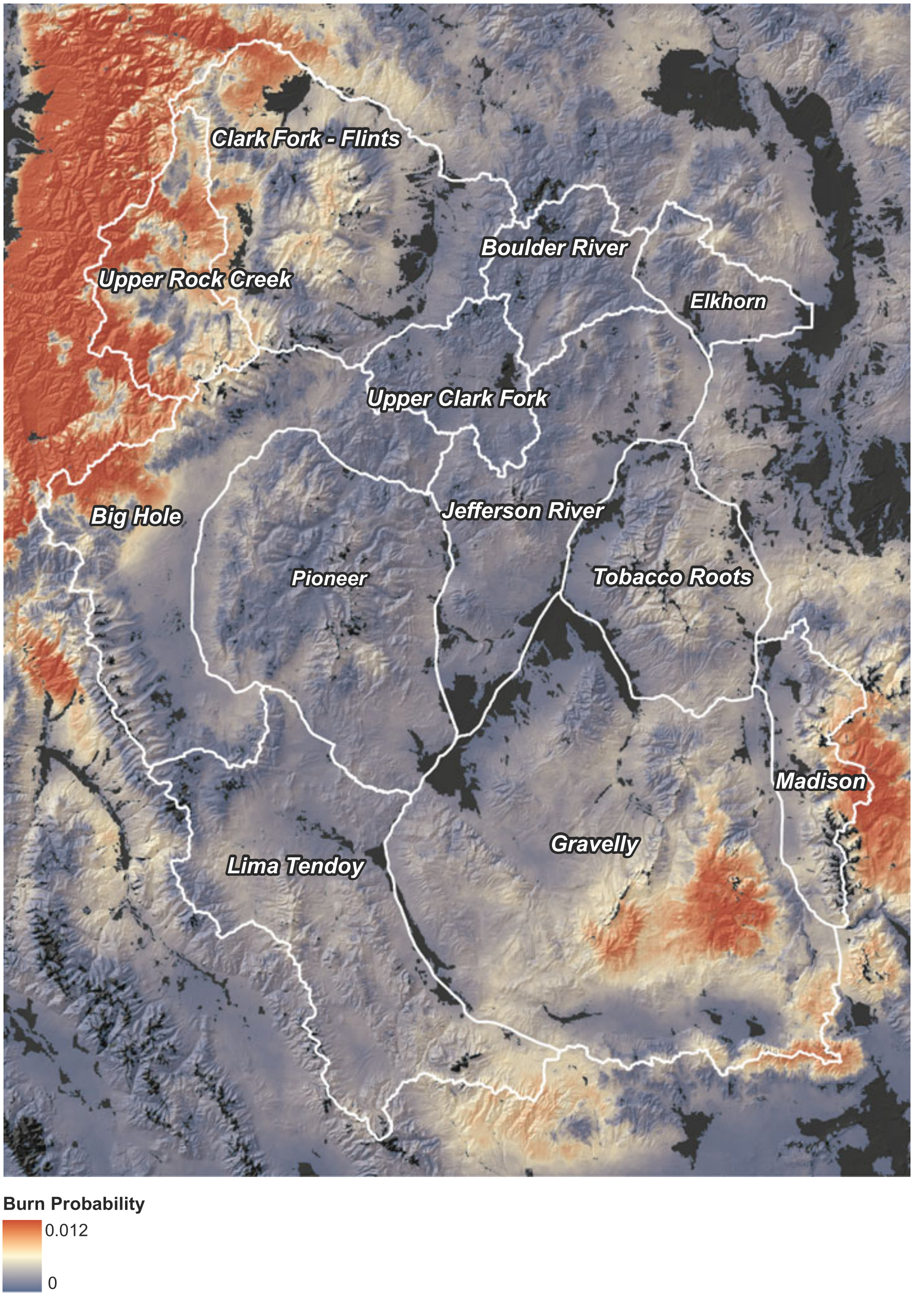

Fig. 5 Map of pixel-level burn probability across the BDNF fire modeling landscape. Burn probabilities range from a high near 0.01 in the NW corner of the area to 0.0002 in the low spread-rate portions of the low ignition density band trending from the SW to the NE corner. *Black* indicates non-burnable areas of the landscape (primarily agricultural land)

Fig. 6 Map of pixel-level mean fireline intensity across the BDNF fire modeling landscape. Mean fireline intensity values range from a high near 56,000 kW/m in intact forested areas to a minimum near 200 kW/m. *Black* indicates non-burnable areas of the landscape (primarily agricultural land)

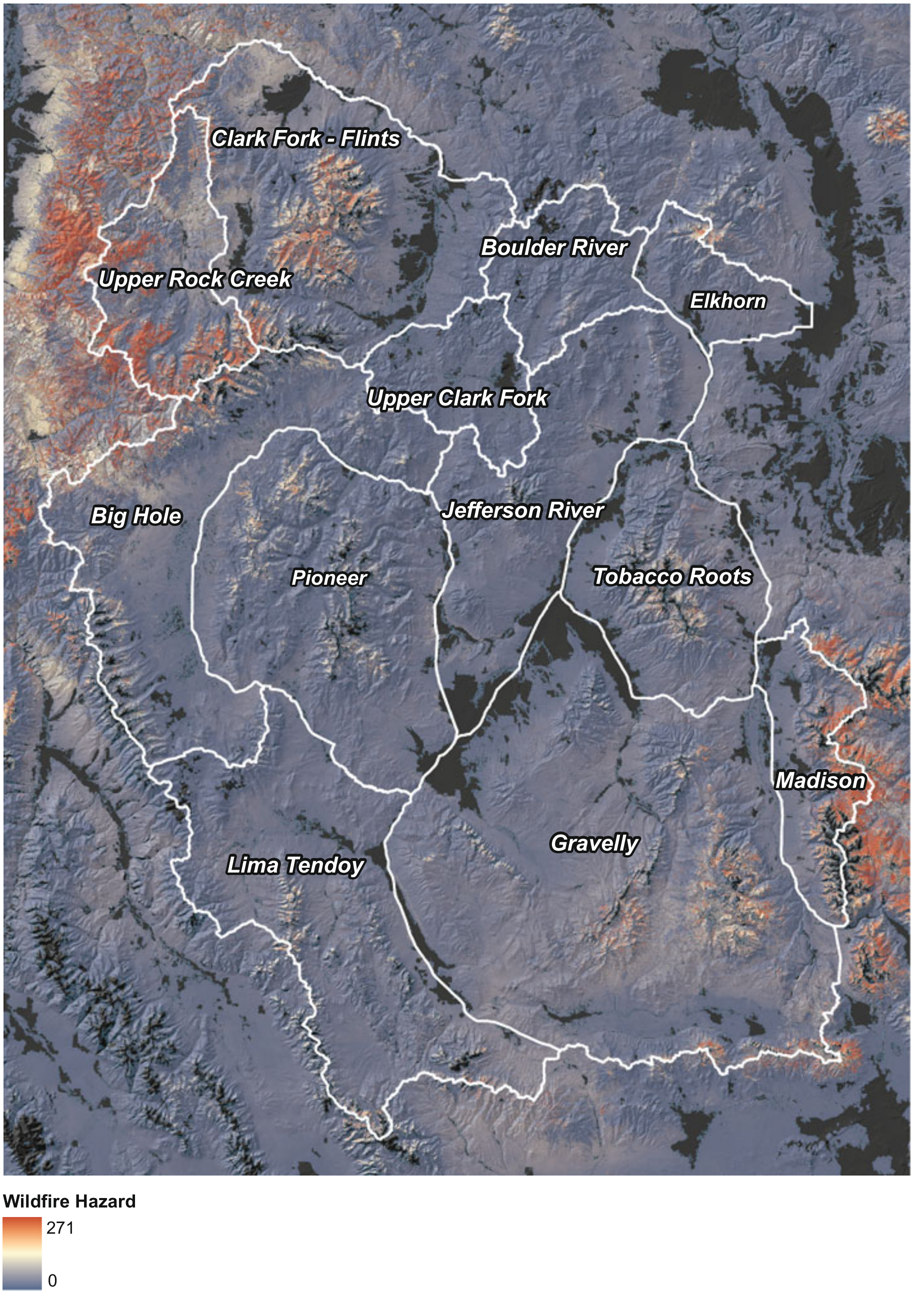

Fig. 7 Map of integrated wildfire hazard across the BDNF fire modeling landscape. Integrated wildfire hazard is the product of BP and MFI. Values of integrated wildfire hazard span nearly six orders of magnitude. The values are highest in the still-intact, crown fire-capable forests of the high BP NW region of the landscape, and lowest in the forests, now prone to low-intensity surface fire and low-grade passive crown fire due to defoliation by beetles, found in the low-probability band trending from the SW to the NE corner

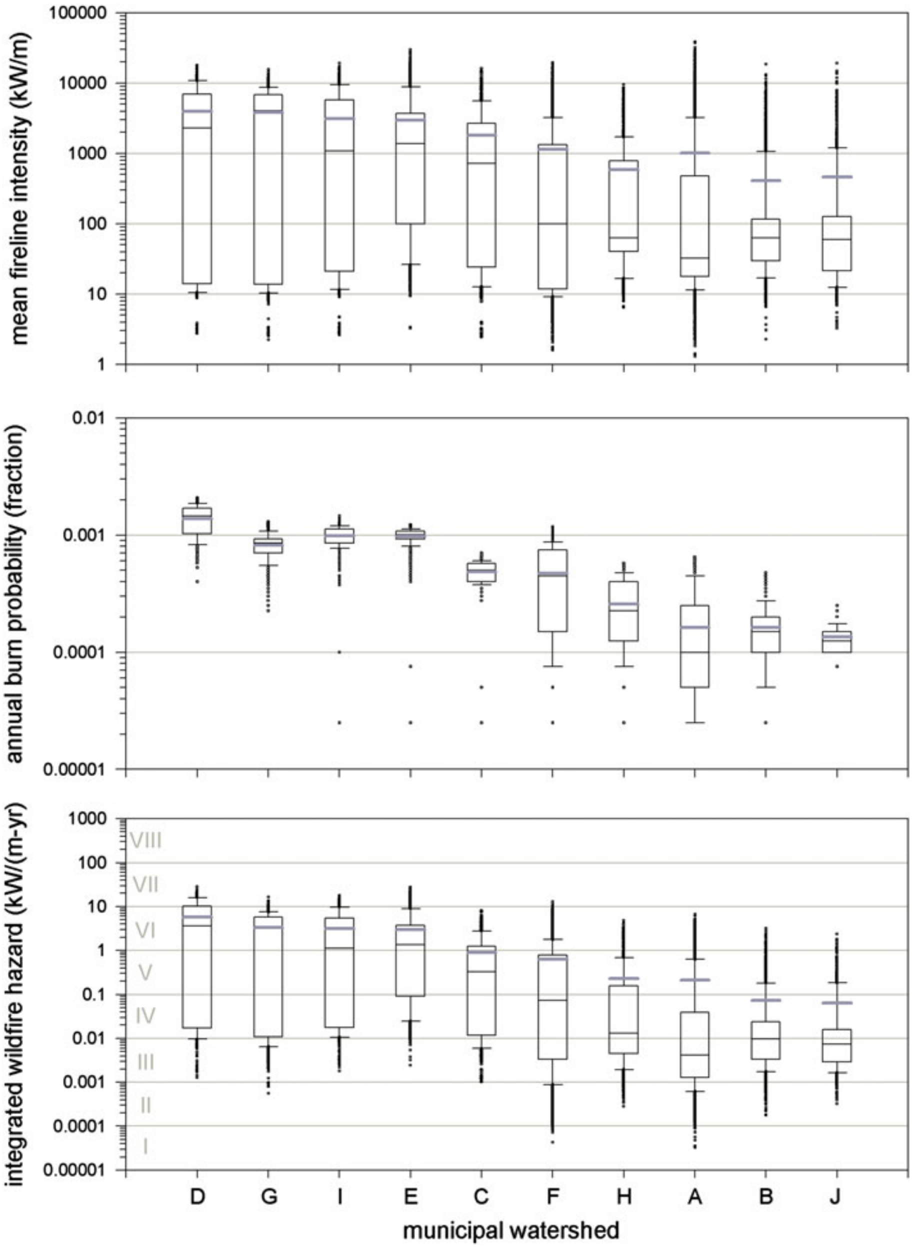

Fig. 8 Box plots of BP, MFI, and integrated hazard for all 10 municipal watersheds, sorted by mean integrated hazard. *Box* plots indicate the quartiles (the *box*), 10th/90th percentiles (whiskers), median (*black line*), mean (*thick gray line*), and individual values outside the 10th/90th percentiles (*dots*)

Fig. 9 Wildfire hazard characteristics chart for two contrasting municipal watersheds. *Gray dots* indicate watershed J (watershed with the lowest integrated hazard); *black dots* indicate watershed D (highest integrated hazard)

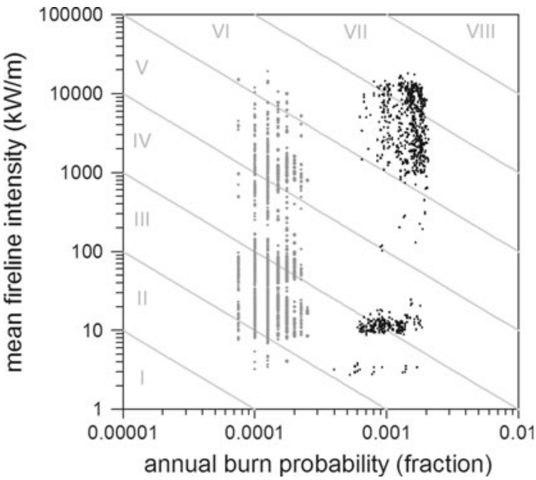

3 Results

Wildfire hazard characteristics vary considerably across the analysis area. The regions of the landscape with the highest annual burn probabilities—the northwest and southeast portions of the landscape (Fig. 5)—exhibit BP values in the range from 0.003 to 0.010. These areas correspond to the regions with the highest ignition density (see Fig. 3). Burn probabilities are lowest in the southwest–northeast band that corresponds to low ignition density. Burn probability in this area ranges broadly from 0.0002 to 0.0010. The range of simulated burn probability values encompasses the non-spatial, historical average annual burn probability of 0.0012.

Table 2 Summary of pixel-based wildfire hazard characteristics within each of the ten municipal watersheds on the Beaverhead-Deerlodge National Forest

(a) Watershed	Mean of burnable pixels			(e) Expected annual area burned (ha/year)
	(b) Burn probability	(c) Mean fireline intensity (kW/m)	(d) Integrated wildfire hazard (kW/(m-year))	
A	0.0001628	1,014	0.2098	1.64
B	0.0001634	409	0.0730	0.51
C	0.0004873	1,827	0.8996	0.25
D	0.0013794	3,952	5.8270	1.00
E	0.0009767	2,980	2.9960	2.44
F	0.0004720	1,142	0.6248	2.80
G	0.0008151	3,858	3.3200	1.29
H	0.0002570	593	0.2298	0.32
I	0.0009899	3,103	3.1151	1.29
J	0.0001347	463	0.0633	0.18

Expected annual area burned (column e) is the product of watershed-mean burn probability (column b) and the burnable watershed area (Table 1, column d). Expected annual area burned as a fraction of the burnable watershed area is therefore equivalent to the watershed-mean burn probability

Forested areas less impacted by the beetles at the time of the analysis, like the Clark Fork-Flints landscape, exhibit higher MFI values than those heavily impacted, such as the Boulder River landscape, where the highest MFI values reach just half that amount (Fig. 6). Valley-bottom grasslands exhibit moderate MFI values relative to much of the beetle-impacted forests, but the intact forests produce the highest MFI values in the fire modeling area. Low MFI values can exist adjacent to areas with high MFI values because of localized fuelbed characteristics. Lastly, the areas of greatest integrated hazard occur where both BP and MFI are high—the still-dense forests of the northwest and southeast corners of the analysis area—where watersheds D, E, G, and I are located (Fig. 7).

Box plots depicting the distribution of BP, MFI, and integrated hazard within each watershed illustrate a large range of variability of wildfire hazard (Fig. 8). Within any given watershed, MFI varies across roughly four orders of magnitude, despite the fact that MFI is itself a pixel mean that masks some variability. Fireline intensity inherently ranges across roughly five orders of magnitude, from a low of 10 kW/m for a backing fire in light fuel to a high of 100,000 kW/m for a fast-spreading crown fire. Burn probability varies across 1–2 orders of magnitude within a watershed. Generally speaking, larger watersheds exhibit greater variability in BP. Because integrated hazard is the product of BP and MFI, and because BP and MFI vary so greatly themselves, integrated hazard varies across 4–5 orders of magnitude. Integrated wildfire hazard is sorted into classes, indexed by roman numerals and partitioned according to the orders of magnitude. Median watershed hazard class values range from class III to class VI, with four watersheds in the highest observed hazard class (D, E, G, and I). Watersheds A, B, and J appear to have the least exposure to wildfire. The variability of integrated hazard within watersheds appears to be largely driven by variation in mean fireline intensity, whereas variation between watersheds appears to be driven largely by burn probability.

The joint distribution of BP and MFI for two contrasting watersheds is depicted in a wildfire hazard characteristics chart (Fig. 9). Watershed J is the watershed with the lowest mean integrated hazard, whereas watershed D has the highest hazard. As seen on this chart and in Fig. 8, their BP values differ by a factor of ten. In contrast, they exhibit a similar overall range of MFI values. Watershed D, however, has a higher concentration of pixels in the upper range of the MFI scale, resulting in a much higher watershed-mean MFI. Figure 9 reveals a bimodal distribution of MFI within watershed D that is not apparent in the box plots, with one cluster of points in the 1,000 to 10,000 kW/m range and another clustered around 10 kW/m. This bimodal distribution is largely a function of the underlying fuelbed. The lower cluster of points is simply not capable of producing high fireline intensity values—it consists of compact forest litter and is found on the lee side of a small lake, causing many fires to flank through this area rather than spread through as a heading fire. The cluster of higher MFI values consists of fuels characterized by litter with a grass component and a forest canopy capable of supporting passive and active crown fire.

Watershed-mean BP values are likewise highly variable (Table 2; column b), varying by an order of magnitude between the highest (watershed D; 0.0013794) and lowest (watershed J; 0.0001347). The non-spatial average annual historical BP is on the higher end with respect to mean watershed BP, suggesting that municipal watersheds are largely located in areas of lower fire hazard relative to the broader landscape. Relative ignition density exhibits fairly high positive correlations with both BP (0.70) and MFI (0.85), highlighting the potential influence of modeled ignition processes on modeled fire growth and behavior.

Mean fireline intensity is similarly variable (Table 2; column c), ranging from a high of 3,952 kW/m in watershed D to a low of 409 kW/m in watershed B. Watershed D has the highest mean integrated wildfire hazard (Table 2; column d), which is not surprising given it ranks highest in both components of integrated hazard (burn probability and fireline intensity). Watershed J, by contrast, has the lowest mean integrated hazard, ranking last in burn probability and second to last in mean fireline intensity. Lastly, watershed F has the highest expected value of annual area burned (Table 2; column e), a function of moderate burn probability (6th highest) and relatively large burnable area (second highest). Expected area burned as a fraction of the watershed size is equivalent to the watershed-mean BP (Table 2, column b).

4 Discussion

The research effort presented here illustrates the application of geospatial analysis, large-fire simulation, and burn probability modeling to examine pixel-based measures of wildfire hazard and watershed exposure. The derivation of an integrated measure of wildfire hazard (product of BP and MFI) provides a useful filter for identifying watersheds that are particularly likely to burn with high intensity and for informing mitigation and prioritization efforts. Thus, a multitude of wildfire hazard and exposure characterizations exist and can jointly inform wildfire risk analyses.

A logical next step would be to analyze potential wildfire consequences to municipal watersheds and post-fire impacts to water quality. Additional spatial variables relevant to watershed health or susceptibility, such as slope steepness and erosive potential could be incorporated into our integrated wildfire hazard index. Associating fireline intensity with primary vegetation type to predict fire severity would improve projection of fire effects; strong erosion response is not necessarily always associated with high flame lengths, especially for herbaceous fuels (Parsons et al. 2010). Rather, post-fire hydrogeomorphic response is strongly correlated with spatial extent and distribution of moderate and high burn severity (Cannon et al. 2010; Gartner et al. 2008; Hyde et al. 2007). Thus, coupling our modeling approach with burn severity models could be particularly informative. We could then further couple estimates of post-fire vegetation removal with slope stability models to estimate changes to landslide susceptibility (Ren et al. 2011).

There are a number of challenges associated with fire effects prediction that could be identified and addressed in future expansions. Estimating resource response to fire can be confounded by complex spatiotemporal dynamics and limited scientific understanding (Keane et al. 2008). Existing models provide useful information on likely first-order fire effects, but some level of inference is still necessary to characterize second-order fire effects (e.g., impacts to water quality) that often are of greater interest to managers (Reinhardt and Dickinson 2010). Approaches adopted in the literature include pairing fire outputs with secondary simulation or process-based models and reliance on expert judgment (Thompson et al. 2011b; Keane and Karau 2010; Ager et al. 2007; Roloff et al. 2005). Embedding additional ecological models may come with costs of increased data demands and propagated uncertainty.

It is important to explicitly recognize modeling assumptions and their potential influence on results. In our case, there are at least two major assumptions to highlight. First, due to a lack of a locally available high-resolution ignition density grid, we assumed a coarser national-scale grid would be sufficient. A comparison of recent ignitions and grid density values (Fig. 3) suggests our assumption is valid, but this may not always be the case. The influence of modeled ignitions on burn probabilities can be substantial, as our results comparing relative ignition density and wildfire hazard characteristics indicated, and further as indicated in recent studies (Parks et al. 2012; Bar Massada et al. 2011). Second, our modeling of the impacts of the beetle infestation on fuel conditions likely influenced results. We modeled the longer-duration gray phase and assumed reduced canopy bulk density and canopy cover, which tended to reduce crown fire potential and mean fireline intensity in affected areas. If fires occur in the near-term red phase, we might expect significantly different fire behavior. The specific impacts of beetles on fuel conditions and fire behavior are an ongoing debate within the fire modeling community (e.g., Moran and Cochrane 2012; Jolly et al. 2012; Simard et al. 2012).

There is also a need to consider the limitations and uncertainties of fire modeling tools. Sullivan (2009a, b, c) offers a comprehensive overview of surface fire spread modeling, highlighting a need to improve basic fire science and to better understand how uncertainty and errors propagate through models. Assumptions and prediction errors related to crown fire potential and propagation, and limited consideration of dynamic fire–atmosphere and fire–fuels interactions are of particular concern (Ager et al. 2011; Cruz and Alexander 2010; Mell et al. 2010). Thus, caution in scope of inference and careful data critiquing and validation is warranted. Output from wildfire simulation models is one the component of a broader set of information used to guide mitigation and restoration planning and can be viewed as a complement to local expertise. With respect to our application, we devoted considerable energy to acquiring, critiquing, and editing geospatial fuels data with attention to guidance (Stratton 2009) and with the assistance of BDNF fire and fuel management staff. FSim has undergone validation efforts at the national scale (Finney et al. 2011), and our modeling results across the landscape studied here indicate agreement with a (limited) historical fire record.

Burn probability modeling is increasingly used across the fire and fuels management continuum. The analytical work presented in this article could inform pre-season planning and fire management plan updating, and in particular has application to fuel management planning. Landscape-scale fuel treatment planning combines risk-based analyses of fuel management needs with identification of feasible management opportunities. Treatment strategy design could seek to interrupt major fire flow paths to reduce likelihood of spread into susceptible watersheds and/or to mitigate fire behavior and burn severity within watersheds. A process of comparative risk assessment could evaluate and rank alternative hazardous fuels reduction strategies in terms of impacts to wildfire hazard and exposure. Prioritizing treatments could additionally be based on relative importance weights assigned to municipal watersheds based upon quantity, demographics, and socioeconomic vulnerability (e.g., Gaither et al. 2011) of population served.

5 Conclusion

This research effort presents novel approaches to characterize wildfire hazard and thereby advances the science of wildfire exposure analysis and risk assessment. Our wildfire hazard and exposure assessment sought to understand where and under what conditions fire is likely to interact with municipal watersheds. Combining spatially explicit information on burn probability and fireline intensity provides useful information for prioritizing mitigation and restoration efforts. The derivation of pixel-based integrated hazard metrics improves our ability to consider the potential ecological and human health impacts associated with wildfire on the landscape. As our ability to understand and model fire effects improves so too will our ability to integrate wildfire hazard analyses into more informative risk analyses that focus on estimating both likelihood and consequences of wildfire.

In our case study of wildfire hazard and exposure on the Beaverhead-Deerlodge National Forest, we developed novel classification systems for wildfire hazard and exposure, and used this system to highlight threatened municipal watersheds. We demonstrated vast differences in fire likelihood, fire behavior, and expected area burned across municipal watersheds. Given the high priority on protecting human life and safety and the subsequent obligation to protect drinking water from wildfire-related degradation, the nature of analysis we present here could have wide application across the nation.

Acknowledgments We would like to thank the staff of the Beaverhead-Deerlodge National Forest, and Kevin Hyde, Tyron Venn, and two anonymous reviewers. The Rocky Mountain Research Station and National Fire Decision Support Center supported this effort.

References

Agee JK (1993) Fire ecology in the Pacific Northwest forests. Island Press, Washington

Ager AA, Finney MA, Kerns BK, Maffei H (2007) Modeling wildfire risk to northern spotted owl (*Strix-occidentaliscaurina*) habitat in Central Oregon, USA. For Ecol Manag 246(1):45–56

Ager AA, Valliant NM, Finney MA (2010) A comparison of landscape fuel treatment strategies to mitigate wildland fire risk in the urban interface to preserve old forest structure. For Ecol Manag 259(8): 1556–1570

Ager AA, Vaillant NM, Finney MA (2011) Integrating fire behavior models and geospatial analysis for wildland fire risk assessment and fuel management planning. J Combust. Article ID 572452, p 19. doi: 10.1155/2011/572452

Ahl R, Weldon H, Vanderzanden D (2010) Rapid response VMPA production for the Beaverhead-Deerlodge national forest with an application of the Random Forest classification algorithm. Version 10.1. USDA Forest Service, Northern Region Engineering Geospatial Services Group, May 2010 (unpublished report) Missoula, MT

Bar Massada A, Radeloff VC, Stewart SI, Hawbaker TJ (2009) Wildfire risk in the wildland-urban interface: a simulation study in northwestern Wisconsin. For Ecol Manag 258:1990–1999

Bar Massada A, Radeloff VC, Stewart SI (2011) Allocating fuel breaks to optimally protect structures in the wildland-urban interface. Int J Wildland Fire 20:59–68

Benda LE, Miller D, Bigelow P, Andras K (2003) Effects of post-wildfire erosion on channel environments, Boise River, Idaho. For Ecol Manag 178:105–119

Bisson PA, Rieman BE, Luce CH, Hessburg PF, Lee DC, Kershner JL, Reeves GH, Gresswell RE (2003) Fire and aquatic ecosystems of the western USA: current knowledge and key questions. For Ecol Manag 178:213–229

Brauman KA, Daily GC, Ka'eo Duarte T, Mooney HA (2007) The nature and value of ecosystem services: an overview highlighting hydrological services. Annu Rev Environ Resour 32:67–98

Brown TC (2000) Economic issues for watersheds supplying drinking water. In: Dissmeyer GF (eds) Drinking water from forests and grasslands: a synthesis of the scientific literature. USDA Forest Service GTR SRS-39. Southern Research Station, Asheville, North Carolina, pp 42–54. Online: http://www.srs.fs.usda.gov/pubs/gtr/gtr_srs039/gtr_srs039.pdf. Accessed August 19, 2010

Brown TC, Binkley D (1994) Effect of management on water quality in North American forests. General Technical Report GTR RM-248. USDA Forest Service Rocky Mountain Forest and Range Experiment Station. Fort Collins, CO

Brown TC, Froemke P (2010) Risk of impaired condition of watersheds containing national forest lands. General Technical Report RMRS-GTR-251. USDA Forest Service Rocky Mountain Research Station, Fort Collins, CO, p 57

Brown TC, Hobbins MT, Ramirez JA (2008) Spatial distribution of water supply in the coterminous United States. J Am Water Res As 44(6):1474–1487

Calkin DE, Hyde KD, Robichaud PR, Jones JG, Ashmun LE, Loeffler D (2007) Assessing post-fire values-at-risk with a new calculation tool. General Technical Report RMRS-GTR-205. USDA Forest Service, Rocky Mountain Research Station, Fort Collins, CO

Calkin DE, Ager AA, Thompson MP (2011a) A comparative risk assessment framework for wildland fire management: the 2010 cohesive strategy science report. General Technical Report RMRS-GTR-262. US Department of Agriculture, Forest Service, Rocky Mountain Research Station, Fort Collins, p 63

Calkin DE, Thompson MP, Finney MA, Hyde KD (2011b) A real-time risk-assessment tool supporting wildland fire decision-making. J For 109(5):274–280

Cannon SH, Gartner JE, Rupert MG, Michael JA, Rea AH, Parrett C (2010) Predicting the probability and volume of post wildfire debris flows in the intermountain western United States. GSA Bull 127–144. doi:10.1130/B26459.1.122

Cruz MG, Alexander ME (2010) Assessing crown fire potential in coniferous forests of western North America: a critique of current approaches and recent simulation studies. Int J Wildland Fire 19(4):377–398

Dennison PE, Cova TJ, Mortiz MA (2007) WUIVAC: a wildland-urban interface evacuation trigger model applied in strategic wildfire scenarios. Nat Hazards 41:181–199

Dunham JB, Rosenberger AE, Luce CH, Rieman BE (2007) Influences of wildfire and channel reorganization on spatial and temporal variation in stream temperature and the distribution of fish and amphibians. Ecosystems 10:335–346

Emelko MB, Silins U, Bladon KD, Stone M (2011) Implications of land disturbance on drinking water treatability in a changing climate: demonstrating the need for 'source water supply and protection' strategies. Water Res 45:461–472

Fairbrother A, Turnley JG (2005) Predicting risks of uncharacteristic wildfires: application of the risk assessment process. For Ecol Manag 211:28–35

Finney MA (1998) FARSITE: fire area simulator—model development and evaluation. USDA Forest Service, Research Paper RMRS-RP-4, p 47

Finney MA (2002) Fire growth using minimum travel time methods. Can J For Res 32(8):1420–1424

Finney MA (2005) The challenge of quantitative risk assessment for wildland fire. For Ecol Manag 211:97–108

Finney MA, Grenfell IC, McHugh CW (2009) Modeling containment of large wildfires using generalized linear mixed-model analysis. Forest Sci 55(3):249–255

Finney MA, McHugh CW, Stratton RD, Riley KL (2011) A simulation of probabilistic wildfire risk components for the continental United States. Stoch Environ Res Risk Assess. doi:10.1007/s00477-011-0462-z

Fire Executive Council (2009) Guidance for implementation of federal wildland fire management policy. 13 Feb 2009. Available at: http://www/nifc/gov/policies/guidance/GIFWFMP.pdf

Gaither CJ, Poudyal NC, Goodrick S, Bowker JM, Malone S, Gan J (2011) Wildland fire risk and social vulnerability in the Southeastern United States: an exploratory spatial data analysis approach. For Policy Econ 13:24–36

Gartner JE, Cannon SH, Santi PM, Dewolfe VG (2008) Empirical models to predict the volumes of debris flows generated by recently burned basins in the Western US. Geomorphology 96:339–354

Hyde K, Woods SW, Donahue J (2007) Predicting gully rejuvenation after wildfire using remotely sensed burn severity data. Geomorphology 86:496–511

Jenkins MJ, Hebertson E, Page WG, Jorgensen CA (2008) Bark beetles, fuels, fires and implications for forest management in the intermountain West. For Ecol Manag 254:16–34

Jolly WM, Parsons R, Varner JM, Butler BW, Ryan KC, Gucker CL (2012) Do mountain pine beetle outbreaks change the probability of active crown fire in lodgepole pine forests? Comment Ecol 93(4):941–946

Keane R, Karau E (2010) Evaluating the ecological benefits of wildfire by integrating fire and ecosystem simulation models. Ecol Model 221:1162–1172

Keane RE, Agee JK, Fule P, Keeley JE, Key C, Kitchen SG, Miller R, Schulte LA (2008) Ecological effects of large fires on US landscapes: benefit or catastrophe? Int J Wildland Fire 17:696–712

LANDFIRE (2010) Homepage of the LANDFIRE Project, US Department of Agriculture, Forest Service; US Department of Interior, [Online]. Available: http://www.landfire.gov, 10 Dec 2010

Mell WE, Manzello SL, Maranghides A, Butry D, Rehm RG (2010) The wildland-urban interface fire problem: current approaches and 214 research needs. Int J Wildland Fire 19:238–251

Miller C, Parisien MA, Ager AA, Finney MA (2008) Evaluating spatially explicit burn probabilities for strategic fire management planning. Trans Ecol Environ 19:245–252

Monitoring Trends in Burn Severity (MTBS) (2010) Homepage of the MTBS multi-year project, US Geological Survey National Center for Earth Resources Observation and Science (EROS); USDA Forest Service Remote Sensing Applications Center (RSAC), [Online]. Available: http://www.mtbs.gov/index.html. Last Update October 2010

Moody JA, Martin DA (2009) Synthesis of sediment yields after wildland fire in different rainfall regimes in the western United States. Int J Wildland Fire 18:96–115

Moran CJ, Cochrane MA (2012) Do mountain pine beetle outbreaks change the probability of active crown fire in lodgepole pine forests? Comment Ecol 93(4):939–941

Neary DG, Ryan KC, DeBano LF (eds) (2005) Wildland fire in ecosystems: effects of fire on soils and water. Gen. Tech. Rep. RMRS-GTR-42-vol 4. USDA Forest Service, Rocky Mountain Research Station, Ogden, UT, p 250

Noonan-Wright EK, Opperman TS, Finney MA, Zimmerman GT, Seli RC, Elenz LM, Calkin DE, Fiedler JR (2011) Developing the US wildland fire decision support system. J Combust. Article ID 168473, p 14. doi:10.1155/2011/168473

Page WG, Jenkins MJ (2007a) Mountain pine beetle-induced changes to selected lodgepole pine fuel complexes within the intermountain region. Forensic Sci 53:507–518

Page WG, Jenkins MJ (2007b) Predicted fire behavior in selected mountain pine beetle-infested lodgepole pine. Forensic Sci 53:662–674

Parise M, Cannon SH (2012) Wildfire impacts on the processes that generate debris flows in burned watersheds. Nat Hazard. doi:10.1007/s11069-011-9769-9

Parks SA, Parisien MA, Miller C (2012) Spatial bottom-up controls on fire likelihood vary across western North America. Ecosphere 3(1):20. Article 12

Parsons A, Robichaud PR, Lewis SA, Napper C, Clark JT (2010) Field guide for mapping post-fire soil burn severity. USDA Forest Service, Rocky Mountain Research Station, RMRS-GTR-243, Fort Collins, CO

Reeves MC, Ryan KC, Rollins MG, Thompson TG (2009) Spatial fuel data products of the LANDFIRE project. Int J Wildland Fire 18:250–267

Reinhardt ED, Dickinson MB (2010) First-order fire effects models for land management: overview and issues. Fire Ecol 6(1):131–142

Ren D, Fu R, Leslie LM, Dickinson RE (2011) Modeling the mudslide aftermath of the 2007 Southern California Wildfires. Nat Hazards 57:327–343

Rieman BE, Hessburg PF, Luce C, Dare MR (2010) Wildfire and management of forests and native fishes: conflict or opportunity for convergent solutions? Bioscience 60(6):460–468

Rocky Mountain Research Station Fire Sciences Laboratory and Systems for Environmental Management (2002) FireFamilyPlus user's guide, version 3.0. US Department of Agriculture, Forest Service, National Fire and Aviation Management Information Systems Team, Boise

Roloff GJ, Mealey SP, Clay C, Barry J, Yanish C, Neuenschwander L (2005) A process for modeling short- and long-term risk the southern Oregon Cascades. For Ecol Manag 211:166–190

Ryan D, Samuels WB (2010) Fire vs. water: a new tool assesses drinking water's risk from wildland fires. Geoworld 23(7):16–20

Shakesby RA, Doerr SH (2006) Wildfire as a hydrological and geomorphological agent. Earth-Sci Rev 74:269–307

Sikder IU, Mal-Sarkar S, Mal TK (2006) Knowledge-based risk assessment under uncertainty for species invasion. Risk Anal 26(1):239–252

Simard M, Romme WH, Griffin JM, Turner MG (2011) Do mountain pine beetle outbreaks change the probability of active crown fire in lodgepole pine forests. Ecol Mongr 81(1):3–24

Simard M, Romme WH, Griffin JM, Turner MG (2012) Do mountain pine beetle outbreaks change the probability of active crown fire in lodgepole pine forests? Reply Ecol 93(4):946–950

Smith HG, Sheridan GJ, Lane PNJ, Nyman P, Haydon S (2010) Wildfire effects on water quality in forest catchments: a review with implications for water supply. J Hydrol 396:170–192

Stratton RD (2009) Guidebook on LANDFIRE fuels data acquisition, critique, modification, maintenance, and model calibration. Gen. Tech. Rep. RMRS-GTR-220. US Department of Agriculture, Forest Service, Rocky Mountain Research Station, Fort Collins, p 54

Sullivan AL (2009a) Wildland surface fire spread modelling, 1990–2007. 1: physical and quasi-physical models. Int J Wildland Fire 18:349–368

Sullivan AL (2009b) Wildland surface fire spread modelling, 1990–2007. 2: empirical and quasi-empirical models. Int J Wildland Fire 18:369–386

Sullivan AL (2009c) Wildland surface fire spread modelling, 1990–2007. 3: simulation and mathematical analogue models. Int J Wildland Fire 18:387–403

Thompson MP, Calkin DE (2011) Uncertainty and risk in wildland fire management: a review. J Environ Manag 92:1895–1909

Thompson MP, Calkin DE, Finney MA, Ager AA, Gilbertson-Day JW (2011a) Integrated national-scale assessment of wildfire risk to human and ecological values. Stoch Environ Res Risk Assess 25(6):761–780

Thompson MP, Calkin DE, Gilbertson-Day J, Ager AA (2011b) Advancing effects analysis for integrated, large-scale wildfire risk assessment. Environ Monit Assess 179(1–4):217–239